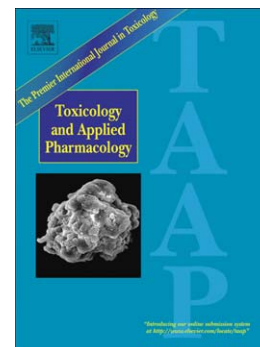# Accepted Manuscript

The antitripanocide benznidazole promotes adaptive response to oxidative injury: Involvement of the nuclear factor-erythroid 2-related factor-2 (Nrf2) and multidrug resistance associated protein 2 (MRP2)

Juan Pablo Rigalli, Virginia Gabriela Perdomo, Nadia Ciriaci, Daniel Eleazar Antonio Francés, María Teresa Ronco, Amy Michele Bataille, Carolina Inés Ghanem, María Laura Ruiz, José Enrique Manautou, Viviana Alicia Catania

Please cite this article as: Rigalli, Juan Pablo, Perdomo, Virginia Gabriela, Ciriaci, Nadia, Francés, Daniel Eleazar Antonio, Ronco, María Teresa, Bataille, Amy Michele, Ghanem, Carolina Inés, Ruiz, María Laura, Manautou, José Enrique, Catania, Viviana Alicia, The antitripanocide benznidazole promotes adaptive response to oxidative injury: Involvement of the nuclear factor-erythroid 2-related factor-2 (Nrf2) and multidrug resistance associated protein 2 (MRP2), *Toxicology and Applied Pharmacology* (2016), doi: 10.1016/j.taap.2016.05.007

The antitripanocide Benznidazole promotes adaptive response to oxidative injury: Involvement of the nuclear factor-erythroid 2-related factor-2 (Nrf2) and multidrug resistance associated protein 2 (MRP2).

Juan Pablo Rigalli[a,d]

Virginia Gabriela Perdomo[a]

Nadia Ciriaci[a]

Daniel Eleazar Antonio Francés[a]

María Teresa Ronco[a]

Amy Michele Bataille[b]

Carolina Inés Ghanem[c]

María Laura Ruiz[a]

José Enrique Manautou[b]

Viviana Alicia Catania[a*]

[a] Institute of Experimental Physiology (IFISE-CONICET). Suipacha 570. (2000) Rosario. Argentina. Phone: +54-341-4305799. FAX: +54-341-4399473.

[b] University of Connecticut, School of Pharmacy, Department of Pharmaceutical Sciences, Storrs, Connecticut, USA. Phone: 860-486-3852. FAX: 860-486-5792.

[c] Institute of Pharmacological Investigations (ININFA-CONICET), University of Buenos Aires, Buenos Aires, Argentina. Phone: +54-11-49616784. FAX: +54-11-4963-8593.

[d] Department of Clinical Pharmacology and Pharmacoepidemiology, University of Heidelberg, Heidelberg, Germany. Phone: +49-6221-56-39400. FAX: +49-6221-56-39402.

* Corresponding author. E-mail: vcatania@fbioyf.unr.edu.ar

Abstract

Oxidative stress is a frequent cause underlying drug-induced hepatotoxicity. Benznidazole (BZL) is the only antitripanocide agent available for treatment of Chagas disease in endemic areas. Its use is associated with side effects, including increases in biomarkers of hepatotoxicity. However, BZL potential to cause oxidative stress has been poorly investigated. Here, we evaluated the effect of a pharmacologically relevant BZL concentration (200 µM) at different time points on redox status and the counteracting mechanisms in the human hepatic cell line HepG2. BZL increased reactive oxygen species (ROS) after 1 and 3 h of exposure, returning to normality at 24 h. Additionally, BZL increased glutathione peroxidase activity at 12 h and the oxidized glutathione/total glutathione (GSSG/GSSG+GSH) ratio that reached a peak at 24 h. Thus, an enhanced detoxification of peroxide and GSSG formation could account for ROS normalization. GSSG/GSSG+GSH returned to control values at 48 h. Expression of the multidrug resistance-associated protein 2 (MRP2) and GSSG efflux via MRP2 were induced by BZL at 24 and 48 h, explaining normalization of GSSG/GSSG+GSH. BZL activated the nuclear erythroid 2-related factor 2 (Nrf2), already shown to modulate MRP2 expression in response to oxidative stress. Nrf2 participation was confirmed using Nrf2-knockout mice in which MRP2 mRNA expression was not affected by BZL. In summary, we demonstrated a ROS increase by BZL in HepG2 cells and a glutathione peroxidase- and MRP2 driven counteracting mechanism, being Nrf2 a key modulator of this response. Our results could explain hepatic alterations associated with BZL therapy.

Keywords

1. Introduction

Intracellular redox status is maintained by the balance between the production of reactive oxygen species (ROS) and the action of enzymatic (e.g. catalase, superoxide dismutase, glutathione reductase) and non-enzymatic antioxidant systems (e.g. reduced glutathione -GSH-, vitamin E, etc.). Oxidative stress arises when the production of ROS exceeds the capacity of the antioxidant systems, which can lead to cellular damage through oxidation of macromolecules and alterations in signal transduction pathways. Although the majority of the intracellular ROS are a natural consequence of aerobic metabolism, xenobiotics are an important source of oxidative stress, either through the release of ROS as by-products of their biotransformation or through direct consumption of antioxidant defenses (Han et al. 2006). It is well known that oxidative stress is associated to the pathogenesis of several liver disorders like alcoholic liver disease, nonalcoholic steatohepatitis, hepatitis C, hepatocellular carcinoma and drug-induced acute liver damage (Han et al. 2006; Cichoz-Lach and Michalak 2014).

Benznidazole (BZL, 2-(2-nitroimidazol-1-yl)-N-(phenylmethyl) acetamide) is the only commercially available drug in endemic countries for the treatment of Chagas disease or American trypanosomiasis. The doses used for the treatment of Chagas disease (5-10 mg/kg b.w., administered for 30-60 days, p.o.) lead to plasma concentrations up to 110 μM (Soy et al. 2015). However, higher intrahepatic concentrations are expected since BZL is orally administered, undergoing first pass effect. The active group of BZL comprises a nitro group, whose metabolism in host cells includes reduction to an amino group which is associated to the generation of reactive intermediaries (e.g. nitro radical) that can further react with oxygen generating superoxide (Wardman 1985; Hall and Wilkinson, 2012). Superoxide is metabolized by superoxide dismutase yielding hydrogen peroxide, which is then detoxified by glutathione peroxidase producing oxidized glutathione (GSSG) or by catalase yielding oxygen and water. Alternatively, superoxide can be scavenged by GSH, also generating GSSG (Winterbourn and Metodiewa 1994). Additionally, under certain conditions, nitro radicals may directly react with GSH consuming the pool of this non-protein antioxidant (Biaglow et al. 1986). Reactivity of BZL metabolites was demonstrated in rat

3

hepatocytes, where exposure to BZL led to oxidative stress determined as an increment in lipid peroxidation (Pedrosa et al. 2001). In addition, increases in biomarkers of hepatotoxicity and liver histopathological alterations have been shown in mice (Strauss et al. 2013) and rats (Rendon 2014) after BZL exposure, possibly associated with oxidative injury. Indeed, Dias Novaes et al. (2015) recently demonstrated an increased in lipid peroxidation and protein carbonylation in BZL-treated mice, thus confirming an association between oxidative stress and hepatic damage. Presently, there are scarce reports analyzing the oxidative potential of pharmacological relevant BZL concentrations in experimental models of human liver. Studies on adaptive mechanisms aimed at counteracting this oxidative injury are also lacking.

Multidrug resistance associated protein 2 (MRP2/ABCC2) is a transporter belonging to the family of the ATP binding cassettes (ABC transporters) expressed in many polarized cells such as hepatocytes, enterocytes, renal tubular cells, among others. It mediates the efflux of endo- and xenobiotics reducing the intracellular burden of potential pro-oxidant compounds (Klaassen and Aleksunes 2010). Moreover, MRP2 extrudes GSSG, which along with *de novo* GSH synthesis contribute to the return to normal GSH levels and redox homeostasis (Hagmann et al. 1999).

MRP2 is frequently modulated at the transcriptional level, being the pregnane X receptor (PXR, NR1I2) a key mediator of its regulation by xenobiotics (Kast et al. 2002). In the absence of an agonist, PXR is predominantly associated to corepressors. Upon agonist binding, for example BZL (Rigalli et al. 2012), PXR dissociates from its corepressors and binds to coactivators, which consequently leads to transcriptional activation of its target genes (Hariparsad et al. 2009). Additionally, the nuclear erythroid 2-related factor 2 (Nrf2) is a transcription factor that plays a key role in orchestrating adaptive responses to oxidative stress. In homeostatic conditions, Nrf2 is anchored to Kelch-like ECH-associated protein 1 (Keap1) in the cytosol. In response to exposure to ROS, electrophilic metabolites or non-oxidizing Nrf2 activating compounds like oltipraz (Maher et al. 2007), Nrf2 dissociates from Keap1, translocates into the nucleus and activates the expression of several target genes by binding to antioxidant response elements (ARE) in their promoters. Among Nrf2 target genes are antioxidant enzymes, the glutamate-cysteine ligase (which catalyzes

4

the rate-limiting step in GSH synthesis) and MRP2. These genes could be pharmacologically activated *via* Nrf2. For instance, it has been demonstrated that administration of an Nrf2 activator to mice ameliorates hepatotoxicity produced by acetaminophen, suggesting a protective role of this transcription factor in drug-induced oxidative stress (Bataille and Manautou 2012).

Although oxidative stress by BZL has been already demonstrated in animal models (Dubin et al. 1984; Pedrosa et al. 2001; Dias Novaes et al. 2015), the only study assessing oxidative stress by BZL in a human hepatic cell line showed no changes in ROS levels (Davies et al. 2014). However, the BZL concentrations employed in that study were lower than the intrahepatic levels that can be attained during BZL treatment under oral administration and first pass effect. Moreover, the study was performed using only a single exposure time point (24 h) and levels of glutathione species were not assessed. Considering that pro-oxidant drugs can trigger increases in ROS rather quickly (Vyas et al. 2005), which can be equally detoxified and disposed of relatively fast, any increment in ROS by BZL followed by an induction of antioxidant systems and/or GSSG extrusion by MRP2 occurring prior to this 24 h time point cannot be ruled out. The aim of the present work was to assess the effect of exposure of HepG2 cells, used as a model of human hepatocyte, to an intrahepatic pharmacologically-relevant concentration of BZL on the intracellular redox balance and the adaptive mechanisms triggered to counteract the oxidative injury at different time points.

5

2. Materials and methods

2.1. Chemicals

Benznidazole (BZL), dithionitrobenzoic acid, oxidized glutathione (GSSH), reduced glutathione (GSH), glutathione, nitroblue tetrazolium, MK571, β-NADPH, riboflavin, rifampicin (RIF), sulfosalicylic acid, tert-butyl hydroperoxide (tBOOH) and 2-vinylpyridine were purchased from Sigma-Aldrich (St. Louis, MO, USA). DMSO and hydrogen peroxide were purchased from Merck (Darmstadt, HE, Germany). All other chemicals were of analytical grade purity.

2.2. Cell culture and treatments

HepG2 cells were used as an *in vitro* model of human hepatocytes since they are easily available and retain structural, functional and biochemical properties observed *in vivo* (Sormunen et al. 1993). Preservation of polarity exhibited by HepG2 cells is essential for the proper localization of apical membrane transporters like MRP2 (Cantz et al. 2000). Moreover, HepG2 cells do not display basal oxidative stress, as seen in hepatocyte primary culture. In addition, HepG2 cells express Nrf2 that showed to be activated by pro-oxidant compunds (Vollrath et al. 2006; Li et al. 2014). HepG2 cells were grown in Dulbecco's modified Eagle's medium (DMEM) and Ham's F-12 medium (Invitrogen, Carlsbad, CA, USA) at a 1:1 proportion supplemented with 10% fetal bovine serum (PAA, Pasching, Austria), 2 mM L-glutamine, antibiotics (5 mg/ml penicillin, 5 mg/ml streptomycin and 10 mg/ml neomycin) and 0,1 mg% insulin (Invitrogen). Cells were incubated at 37°C in a humidified atmosphere containing 5% CO_2 as described (Rigalli et al. 2015). Unless otherwise stated, treatments were performed in 6-well plates. For this purpose, cells were collected by trypsinization and seeded at a density of $5x10^5$ cells/well. BZL was dissolved in DMSO and added to the culture medium from a 1000x stock solution to reach a final concentration of 200 µM. This concentration was selected taking into account that plasma concentrations in BZL-treated patients reach up to 110 µM (Soy et al. 2015) and that preliminary experiments in rats showed BZL intraportal concentration up to 3-fold the systemic plasma levels (see Supplementary Material).

6

Cells were incubated with BZL for 15 min, 1 h, 3 h, 24 h and 48 h depending on each particular experiment. Only DMSO (0.1% v/v) was added to control cells (C). Tert-butyl hydroperoxide (tBOOH, 500 µM, 15 min) was used as a positive control of reactive oxygen species (ROS) generation (Toledo et al. 2014). The concentration-dependence of BZL effects on intracellular redox status was evaluated incubating the cells with BZL 50, 100 and 200 µM for 24 h. Then, glutathione levels were quantified as described below.

2.3. Redox status

2.3.1. Intracellular ROS measurement

Intracellular ROS generation by BZL was assessed by quantification of dichlorodihydrofluorescein diacetate (DCFH-DA) oxidation (Ferretti et al. 2012). After BZL treatment, culture medium was removed, cells were rinsed twice with PBS and further incubated with a solution of DCFH-DA (5 µM) in PBS for 30 minutes. Then, medium was removed; cells were rinsed twice with PBS, scraped in a sucrose solution (0.30 M) and lysed by sonication. Fluorescence (λ_{exc} = 488 nm, λ_{em} = 525 nm) was quantified in cell lysates and represents a measure of intracellular ROS levels. Results were normalized to protein concentration in the cell extracts (Lowry et al. 1951).

2.3.2. Glutathione measurement

The ratio of oxidized glutathione:total glutathione (GSSG/GSSG+GSH) was quantified by the enzymatic recycling procedure of Tietze (1969), as modified by Griffith (1980), which is based on the glutathione catalyzed formation of thionitrobenzoic acid (TNB). For this purpose, cells were rinsed with PBS, scraped with PBS-EDTA (6.30 mM) buffer pH 7.50 and lysed by sonication. Then, samples were deproteinized by addition of sulfosalicylic acid 10% (w/v) in a necessary volume to reach a dilution 1:2 (v/v) in the sample. Following, samples were centrifuged for 5 min (10000 rpm, 4°C). Supernatants were divided in two fractions. One fraction was directly used for the determination of total glutathione (GSSG+GSH); the other fraction was further derivatized to mask GSH thus allowing quantification of only GSSG. Derivatization was performed by incubation with 2-

7

vinylpyridine (3% v/v) in the presence of triethanolamine (5% v/v) for 1 h at 30°C. Reaction medium for glutathione quantification consisted of PBS-EDTA (6.30 mM) buffer pH 7.50, β-NADPH (0.21 M), DTNB (0.60 mM) and glutathione reductase (0.50 units/reaction) in a final volume of 1 ml. The rate of formation of TNB (30°C) was quantified at 412 nm and is indicative of the concentration of glutathione species in the sample.

2.4. Antioxidant enzymes

Cell lysates were obtained by sonication in a PBS-EDTA (6.30 mM) buffer, pH 7.40. Lysates were cleared by centrifugation (10 min, 1000 g) and supernatants were used for activity determinations. Enzyme activities were normalized to the protein concentration of the samples as quantified by the Lowry method (Lowry et al. 1951).

2.4.1. Catalase activity (CAT)

CAT activity was quantified in cell lysates as described by Fina et al. (2014). The method is based on the consumption of hydrogen peroxide in a reaction medium of PBS-EDTA (6.30 mM) pH 7.00 and hydrogen peroxide 0.02 M as substrate. The rate of consumption was monitored at 240 nm.

2.4.2. Superoxide dismutase (SOD) activity

SOD activity was quantified using the method described by Frances et al. (2007) based on the SOD-mediated prevention of the photochemical reduction of nitroblue tetrazolium. Equal amounts of protein were separated using native polyacrylamide gels. After electrophoretic run, gels were equilibrated by incubation in a K_3PO_4 (50 mM)-EDTA (1 mM) buffer, pH 7.80 for 30 minutes. SOD was detected by soaking the gels in equilibration buffer supplemented with 0.24 mM nitroblue tetrazolium, 33.2 μM riboflavin and 0.20 % (v/v) TEMED for 30 minutes. Gels were then illuminated for 10 minutes and SOD was identified as clear bands in uniformly blue colored gels. SOD activity was quantified by measuring the optical density of the corresponding bands using the Gel-Pro 3.0 software (Media Cybernetics, Silver Spring, MD, USA).

2.4.3. Glutathione reductase activity (GRx)

GRx measurement is based on the oxidation of NADPH to NADP coupled to the reduction of GSSG to GSH (Rice et al. 2005). Reaction medium consisted of PBS-EDTA (6.30 mM) pH 7.40, 300 µM NADPH and 500 µM GSSG, 37°C. Reactions were started by addition of cell lysates and consumption of NADPH was followed kinetically at 340 nm.

2.4.4. Glutathione peroxidase (GPx)

GPx was quantified in cell lysates as described by Fina et al. (2014) following the GRx catalyzed consumption of NADPH coupled to the GPx catalyzed reaction of H_2O_2 with GSH. Reactions were performed in a buffer consisting of KH_2PO_4/K_2HPO_4 (50 mM), EDTA (1 mM) pH 7.40 supplemented with 1 mM NaN_3, 200 µM NADPH, 1 mM GSH and 1 U/ml glutathione reductase. Reactions were started by addition of H_2O_2 (0.25 mM) and followed during 30 s at 340 nm.

2.5. Oxidized glutathione efflux

Efflux of GSSG from HepG2 cells was quantified in BZL treated (200 µM, 24 and 48 h) and control cells. For this purpose, cells were treated as described in 2.2. GSSG extruded into culture medium was quantified in the presence or absence of MK571 (10 µM), a MRP inhibitor (Rigalli et al. 2015) during the last 24 h of treatment. Cell viability did not show changes during the efflux period, as determined through MTT assay (data not shown). Aliquots of culture medium were deproteinized by addition of sulfosalicylic acid 10% (w/v) in the necessary volume to reach a 1:2 (v/v) dilution. Samples were then centrifuged for 5 min (10000 rpm, 4°C) and supernatants were derivatized by incubation with 2-vinylpyridine (3% v/v) in the presence of triethanolamine (5% v/v) for 1 h at 30°C. Reaction medium for GSSG quantification consisted of PBS-EDTA (6.30 mM) buffer pH 7.50, β-NADPH (0.21 M), DTNB (0.60 mM) and glutathione reductase (0.50 units/reaction) in a final volume of 1 ml. The rate of formation of TNB (30°C) was quantified at 412 nm and is indicative of the concentration of GSSG in the sample. tBOOH (500 µM, 15 min) was used as a positive control of ROS generation without MRP2 induction and GSSG extruded during

9

24 h after exposure to tBOOH was quantified as above described.

2.6. RNA interference

PXR expression was experimentally diminished using a small interference RNA (siRNA) as described in Rigalli et al. (2011). Briefly, HepG2 cells (5×10^4 cells/well) were seeded in 24-well plates, cultured for 24 h and then transfected by incubation for 48 h with PXR siRNA (h) (Santa Cruz Biotechnology, Santa Cruz, CA, USA; sc-44057, PXR$^-$ cells) or a non-targeting siRNA (Santa Cruz Biotechnology, sc-37007, PXR$^+$ cells), as a control. Both siRNAs were used at a concentration of 100 nM. Dharmafect4 (GE Life Sciences, Lafayette, CO, USA) was used as transfection reagent. Then, knock down was verified at the protein level quantifying PXR expression in total lysates of PXR$^+$ and PXR$^-$ cells. After transfection, siRNA containing medium was removed, cells were rinsed and fresh medium with BZL (200 µM) or vehicle were added. Cells were further incubated for 24 h and MRP2 expression was assessed as described following. Decrease of PXR activity in the knock-down model was further verified by incubation of PXR$^+$ and PXR$^-$ cells with RIF (PXR agonist, 20 µM) (Lehmann et al. 1998) and quantification of CYP3A4 protein expression (known PXR target) as described below.

Nrf2 expression was silenced using ON-TARGET Human NFE2L2 siRNA SMARTpool (GE Healthcare Europe, Freiburg, BW, Germany) at a 100 nM concentration with Dharmafect4 as transfection reagent as described for PXR silencing (Nrf2$^-$ cells). Alternatively, cells were transfected with a non-targeting siRNA (Santa Cruz Biotechnology, sc-37007, Nrf2$^+$ cells). Nrf2 knock-down was assessed through western blot as described following. To assess Nrf2 participation in MRP2 regulation by BZL, transfected cells were incubated with BZL (200 µM, 24 h). Then, MRP2 protein expression was assessed.

2.7. Western blot studies

MRP2 expression was evaluated in cell lysates as described in Rigalli et al. (2012). Briefly, cells were treated with BZL as described in 2.2. After treatment, cells were scraped with RIPA

10

buffer (Thermo Scientific, Rockford, IL, USA), passed 20 times through a 25G needle to facilitate cell lysis and subjected to protein concentration assay (Lowry et al. 1951). Lysates were then used for MRP2 immunoquantitation as described (Rigalli et al. 2012). For nuclear translocation assays, Nrf2 expression was analyzed in nuclear and cytosolic fractions. Samples were processed as described by Ramyaa et al. (2014) and Kang et al. (2003). Briefly, BZL treated (3, 24 and 48 h, 200 µM) or control cells were scraped with cold PBS, centrifuged (5 min, 300 g, 4°C) and resuspended in a lysis buffer consisting of HEPES 10 mM pH 7.50, NaCl 150 mM, Triton X-100 0.6 % (v/v), EDTA 1 mM, DTT 5 mM and phenylmethylsulfonyl fluoride 17 µg/ml and leupeptin 15 µg/µl as protease inhibitors. Cells were incubated in lysis buffer for 20 min and centrifuged (15 min, 14000 rpm, 4°C). The resulting supernatant represents the cytosolic fraction, whereas pellets were further resuspended and incubated for 30 min in a hypertonic buffer consisting of HEPES (20 mM, pH 7.90), NaCl 420 mM, $MgCl_2$ 15 mM, EDTA 0.20 mM, DTT 5 mM and protease inhibitors as described for the lysis buffer. Following, samples were centrifuged (10 min, 15800 g, 4°C). Resulting supernatants represent the nuclear fraction. Protein concentration was quantified by the Lowry method (Lowry et al. 1951). Both fractions were subjected to SDS-PAGE and western blotting as described in Rigalli et al. (2012). Glyceraldehyde-3-phosphate dehydrogenase (GAPDH) and histone H1 were used as loading controls for cytosolic and nuclear fraction, respectively. PXR and Nrf2 silencing as well as CYP3A4 induction by RIF were verified assessing the protein expression in total cell lysates. Primary antibodies were anti-CYP3A4, clone F24P2B10 (Millipore, Darmstadt, HE, Germany); anti-MRP2, M2-III-6 (Enzo Life Sciences, Farmingdale, NY, USA); anti-Nrf2, H-300; anti-PXR, N-16; anti-Histone H1, AE4; anti-GAPDH, FL-335 (Santa Cruz Biotechnology) and anti-β-actin (Sigma-Aldrich). HRP-conjugated goat anti-Mouse IgG (H+L) was used as secondary antibody for anti-CYP3A4, anti-Histone H1, anti-β-actin and anti-MRP2, whereas a HRP-conjugated donkey anti-Rabbit IgG (H+L) (Thermo Scientific, Rockford, IL, USA) was used as secondary antibody for Nrf2 and GAPDH. HRP-conjugated donkey anti-goat IgG (Santa Cruz Biotechnology) was used as secondary antibody for PXR. Detections were performed through chemiluminescence using the ECL Western Blotting substrate (Thermo Scientific).

11

2.8. Reporter gene assay

Nrf2 activation by BZL was further verified using the pGL3-ARE reporter plasmid expressing firefly luciferase under the control of a regulatory sequence bearing an ARE element. pGL3-ARE was a kind gift from Dr. Nathan J. Cherrington (University of Arizona, USA) (Canet et al. 2015). For reporter gene assays, cells were seeded in 96-well plates at a density of 10^4 cells/well, incubated for 24 h and transfected with 0.10 µg/well of pGL3-ARE using 0.30 µl/well of Lipofectamine3000 transfection reagent (Invitrogen) following manufacturer's instructions. Twenty-four hour after transfection mixture addition, cells were rinsed and exposed to BZL (200 µM) or vehicle for 3, 24 or 48 h. Finally, firefly luciferase activity was quantified using Dual-Glo Luciferase Assay System according to manufacturer's instructions (Promega, Fitchburg, WI, USA) with a LD-400 luminometer (Beckman-Coulter, Brea, CA, USA).

2.9. Experiments with Nrf2$^{-/-}$ mice

Male C57BL/6 (wild type, Nrf2$^{+/+}$) mice were purchased from Charles River Laboratories (Wilmington, MA, USA). Original Nrf2$^{-/-}$ (C57BL/6 congenic) breeding pairs were kindly provided by Dr. Angela Slitt (University of Rhode Island). A colony of these Nrf2$^{-/-}$ mice is maintained at The University of Connecticut. All mice were housed in a 12 h dark/light cycle in a temperature and humidity controlled environment and fed normal chow and water *ad libitum* throughout the study (Ghanem et al. 2015). This work was conducted under the University of Connecticut's Institutional Animal Care and Use Committee approved protocol number A12-050. BZL (200 mg/kg b.w./day; dissolved in DMSO:propylene glycol, 2:13 v/v) was administered i.p. for 3 consecutive days to 18-week-old wild type and Nrf2 knock out mice. Control mice were injected with vehicle according to the same schedule. BZL dose was scaled from a previous study in rats in which we observed Mrp2 induction (Perdomo et al. 2013) based on the body surface area of both species (Reagan-Shaw et al. 2012). Twenty-four hours after the last BZL injection mice were sacrificed by decapitation and livers were excised, rinsed in ice-cold saline solution and snap-frozen in liquid nitrogen. Total RNA was extracted from liver using TRIzol reagent (Life Technologies, Carlsbad, CA, USA) following the manufacturer's instructions. cDNA was synthesized using a M-MLV RT Kit (Life Technologies). The

12

expression of Abcc2 was quantified with SYBR green using specific primers by the ΔΔCt method and normalized to the expression of β-actin as housekeeping gene using an Applied Biosystems 7500 Fast Real-Time PCR system as described (Ghanem et al. 2015). Results were expressed as percentage of the control within each group.

2.10. Statistical Analysis

Data are presented as mean ± S.D. Statistical analysis were performed through the Student's t-test or one way ANOVA followed by Newman-Keuls post hoc test for experiments with two or more than two experimental groups, respectively. Significance was set at $p < 0.05$.

3. Results

3.1. Modulation of the redox status by BZL treatment in HepG2 cells.

BZL-treated cells (200 µM) exhibited a time-dependent increase in intracellular ROS levels, which became significant at 1 h (+40%), reaching a peak at 3 h (+57%) and returned to normality by 24 h. Incubation with tBOOH (500 µM, 15 min) exerted an increase in ROS (+35%) as expected (Fig. 1a). The GSSG/GSSG+GSH ratio increased in BZL-treated cells with respect to control cells (+31, +37 and +43% at 1, 3 and 24 h of exposure respectively, Fig. 1b). After 48 h of treatment, this ratio returned to control values. Analysis of the individual components showed an increase in the amount of GSSG as the main reason underlying the imbalance in the glutathione couple (Fig. 1c). Total intracellular glutathione (GSSG+GSH), which results from the balance between *de novo* GSH synthesis and GSSG and GSH extrusion, was not modified at any time point (Fig. 1d). Exposure to tBOOH, used as a positive control for oxidative stress generation, showed the expected pattern of increase in GSSG/GSSG+GSH ratio due to an increase in the amount of GSSG generated (Figs. 1b and 1c).

To assess whether BZL could also trigger a redox disbalance at lower concentrations, GSSG/GSSG+GSH ratio was quantified after 24 h of exposure to different BZL concentrations. No significant changes were observed at 50 and 100 µM. Incubation with 200 µM showed a significant increase in GSSG/GSSG+GSH (+81%, Fig. 1e), agreeing well with data obtained from time-dependence study (Fig. 1b).

3.2. Activation of compensating mechanisms after BZL caused oxidative injury in HepG2 cells.

Activity of catalase (CAT), superoxide dismutase (SOD), glutathione reductase (GRx) and glutathione peroxidase (GPx) were quantified at 12 and 24 h after BZL exposure as possible mechanisms mediating the return to control values of ROS levels and GSSG/GSSG+GSH ratio

14

observed at 24 and 48 h, respectively. Results showed only a significant increase in GPx activity (+66%) at 12 h. No significant differences in the activity of other antioxidant enzymes were observed at either time point (Table 1).

Considering that BZL (200 µM, 48 h) has been shown to induce the expression of MRP2 (+75%), the main GSSG efflux carrier in HepG2 cells (Rigalli et al. 2012), a protective role for this transporter appears to be a probable compensatory mechanism against BZL-triggered redox imbalance. The higher expression of MRP2 in BZL-treated cells at 48 h was corroborated in the present study. Moreover, we found here a significant induction of MRP2 expression by BZL after 24 h of exposure (+68%, Fig. 2a). In accordance with these observations, efflux assays showed a higher excretion of GSSG in BZL-treated cells in comparison to control cells (169 ± 43 and 184 ± 9 at 24 and 48 h, respectively vs C: 100 ± 12 %) (Fig. 2b). These increases were prevented by addition of the MRP2 inhibitor MK571 (10 µM), thus confirming the participation of MRP2 in the enhanced GSSG efflux. Cells exposed to tBOOH, although exhibiting increased intracellular GSSG levels (Fig. 1c), did not show higher GSSG efflux (Fig. 2b) clearly indicating a major role of MRP2 induction rather than the intracellular substrate availability in GSSG elimination by BZL treatment.

3.3. PXR participation in MRP2 induction by BZL (24 h)

Our previous work demonstrated the participation of PXR as mediator of MRP2 induction by BZL (200 µM, 48 h). To elucidate if PXR also contributes to the observed MRP2 induction after only 24 h of treatment with BZL, we now analyzed protein expression in cells with normal PXR expression (PXR^{+} cells) and with reduced PXR expression through transfection with a specific siRNA (PXR^{-} cells). PXR silencing in PXR^{-} cells was verified through western blot (Fig 3a). Furthermore, decrease of PXR function in PXR^{-} cells was confirmed assessing CYP3A4 protein expression after exposure to the typical PXR agonist RIF (20 µM, 24 h). As expected, RIF induced CYP3A4 in PXR^{+} cells (+54%, Fig 3b). No significant changes were observed in RIF-treated PXR^{-} cells, confirming reduction of PXR function in knock-down cells. Under these conditions, BZL (200

15

µM, 24 h) induced MRP2 expression not only in PXR^{+} cells but also in PXR^{-} cells (Fig. 3c) arguing against a major PXR role in the early induction of MRP2 observed at 24 h.

3.4. Nrf2 activation by BZL in HepG2 cells.

Considering that BZL produces an increase in ROS at shorter treatment times and that MRP2 is among the genes regulated by Nrf2, it now appears that Nrf2 is the most likely transcription factor mediating BZL's effect on the transporter expression after 24 h of treatment. Additionally, Nrf2 may regulate the expression and activity of other antioxidant enzymes. Thus, the role of Nrf2 as mediator of the adaptive response to BZL was first assessed by quantifying its translocation to the nucleus, a commonly measured indicator of its activation. Nuclear and cytosolic protein enrichment is shown in Fig. 4a. Significant increases in nuclear levels of Nrf2 were observed at 24 and 48 h of BZL treatment (+204 and +89%, respectively, Fig. 4b), whereas cytosolic levels showed no changes at 3 and 24 h, with a significant decrease (-36%) detected at 48 h (Fig. 4c). Nrf2 activation by BZL was further confirmed using an ARE reporter gene assay. Indeed, a pattern similar to that seen for Nrf2 nuclear translocation was observed with the ARE reporter assay which showed a significant increase (+42%) only at 24 h of BZL exposure (Fig. 4d). The absence of Nrf2 activation at 48 h time-point agrees well with a minor role of Nrf2 in MRP2 regulation by BZL at later time points once redox homeostasis was recovered. In line with these results, MRP2 induction at 48 h could be easily explained considering PXR activation at this later time-point (Rigalli et al. 2012). For a final confirmation of Nrf2 participation in MRP2 regulation by BZL in HepG2 cells, induction assays were repeated in Nrf2^{+} and Nrf2^{-} cells (transfected with a pool of specific siRNAs against Nrf2 and a non-silencing siRNA, respectively). Knock-down was verified by western blot. Indeed, Nrf2^{-} cells exhibited a significant decrease in Nrf2 expression (-79%, Fig 4e). Moreover, while Nrf2^{+} cells showed an increased MRP2 expression by BZL (200 µM, 24 h) (+50%, Fig 4f), agreeing well with previous results (Fig 2), MRP2 induction was abolished in Nrf2^{-} cells, where on the contrary a decrease in MRP2 expression by BZL was observed (-46%, Fig 4f).

16

3.5. *Role of Nrf2 in Mrp2 induction by BZL in vivo.*

To test that Nrf2 activation by BZL mediates the MRP2-driven adaptive response to oxidative injury produced by BZL in an *in vivo* model, hepatic Mrp2 expression was quantified at the mRNA level after treatment of wild type ($Nrf2^{+/+}$) and knockout ($Nrf2^{-/-}$) mice with BZL. In wild type mice results showed an induction of hepatic Mrp2 (+194%) by BZL with respect to control mice (Fig. 5). No induction by BZL was observed in $Nrf2^{-/-}$ mice (Fig. 5).

4. Discussion

Oxidative stress arises when ROS production exceeds the antioxidant defenses of the cell. This can lead to chemical, and finally, functional modifications to cellular macromolecules, ultimately impairing cellular homeostasis (Han et al. 2006). Oxidative stress-mediated drug hepatotoxicity is well known (Gu and Manautou 2012). The antitripanocide BZL has been shown to cause oxidative stress in rodent liver (Pedrosa et al. 2001; Rendon 2014; Dias Novaes et al. 2015). However, the antioxidant mechanisms responsible for counteracting this redox imbalance have not been defined. Additionally, an increase in serum alanine transaminase as hepatotoxicity marker was observed in mice (Davies et al. 2014; Dias Novaes et al. 2015), rats (Perdomo et al., unpublished results) and also in patients treated with BZL (Viotti et al. 2009). Up to date, the only study dealing with BZL-triggered oxidative stress in a model of human hepatocytes failed to show an increase in ROS by BZL treatment (Davies et al. 2014). However, concentrations employed were lower than those that could be reached intrahepatically during BZL *in vivo* treatment and ROS were measured at only a single, late time point. Here, we have quantified ROS generation and the GSSG/GSSG+GSH ratio as markers of oxidative stress at different exposure times to 200 µM of BZL. Our findings showed a time-dependent increase in ROS that can be generated during biotransformation of the BZL nitro group (Wardman 1985; Hall and Wilkinson 2012). The return to ROS basal levels was coupled to an increase in GSSG/GSSG+GSH ratio due to an enhancement in GSSG levels without changes in total glutathione. Improved H_2O_2 detoxification capacity by increased GPx activity can explain ROS clearance between 3 and 24 h of BZL exposure with a concomitant increase in GSSG formation. A direct reaction of superoxide (Winterbourn and Metodiewa 1994) or BZL derived nitro radicals with GSH (Biaglow et al. 1986) may also explain ROS clearance and GSSG increases.

MRP2/ABCC2 is an organic anion transporter expressed in different epithelial cells including hepatocytes. It transports GSH and more efficiently GSSG (Hagmann et al. 1999) playing a key role in glutathione and redox homeostasis and contributing to reduce the intracellular GSSG

burden without NADPH consumption. Our results here showed that BZL produces an increase in GSSG/GSSG+GSH due to an enhanced GPx activity and probably due to direct GSH oxidation by ROS and BZL reactive intermediaries. A return of this ratio to control levels was seen after 48 h. As no changes in GRx activity by BZL were observed, an increased GSSG efflux appeared to be the most likely mechanism to explain our findings. In our previous work we observed an increase in MRP2 expression in HepG2 cells after 48 h of BZL exposure (Rigalli et al. 2012). Here we also showed MRP2 induction at an earlier time point (24 h) that could explain the decrease in GSSG/GSSG+GSH and intracellular GSSG levels between 24 and 48 h of BZL treatment. To further test this hypothesis, we quantified GSSG efflux into the culture medium after 48 h of BZL treatment. The results showed indeed an increased GSSG extrusion in BZL-treated cells that was prevented by the MRP2 inhibitor MK571. GSSG efflux was not increased when cells were only incubated with tBOOH, a situation resembling ROS and GSSG increases by BZL (Toledo et al. 2014) but not associated to MRP2 induction (unpublished results). Thus, enhanced MRP2 expression and not higher substrate availability seems to play the most important role in GSSG clearance in conditions of BZL-triggered oxidative stress.

PXR is a known mediator of MRP2 regulation by xenobiotics (Kast et al. 2002). Moreover, we have demonstrated its participation in MRP2 induction by BZL after 48 h of treatment and that BZL was able to activate PXR (Rigalli et al. 2012). To test whether PXR is also mediating the MRP2 induction by BZL at the earlier time point of 24 h, we knocked down PXR protein expression. Unlike previous results at 48 h, PXR silencing did not prevent MRP2 induction by BZL at 24 h, clearly suggesting a negligible role of this nuclear receptor at this shorter incubation time.

Nrf2 has been identified as a key regulator of adaptive responses to oxidative injury. Under homeostatic conditions, it is anchored in the cytosol by interaction with Keap1. Upon activation by enhanced ROS production or electrophilic conditions, Nrf2 dissociates from Keap1, migrates into the nucleus and activates the expression of target genes by binding to ARE elements in the promoter of target genes (Bataille and Manautou 2012). Nrf2 has been shown to modulate the expression of antioxidant enzymes (Noh et al. 2015) and Mrp2 (Ghanem et al. 2015) after

19

treatment with toxic acetaminophen doses in animal models. We report here for the first time a time-dependent stimulation of nuclear Nrf2 translocation by BZL that represents a clear evidence of Nrf2 activation and strongly suggests a role of Nrf2 in the regulation of antioxidant systems and MRP2 by BZL. The reduction of nuclear Nrf2 at 48 h although not enough to return to basal levels in control cells, may be attributed to the decrease in intracellular ROS and GSSG levels at this time point. Surprisingly, cytosolic Nrf2 levels declined at 48 h of BZL exposure. However, a reduction in Nrf2 expression has been already reported during treatment with other electrophiles, such as diethylmaleate (Itoh et al. 2003). The functional relevance of increased nuclear Nrf2 protein localization was confirmed assessing the activity of a reporter gene under the control of an ARE element. As expected, BZL increased reporter gene activity at the same time point when maximum Nrf2 accumulation was detected, showing Nrf2's ability to transactivate target genes. Although MRP2/Mrp2 regulation by Nrf2 has been already demonstrated (Ghanem et al. 2015) and our results provide clear evidence of Nrf2 activation by BZL, a loss-of-function-experimental approach would provide the ultimate evidence linking Nrf2 as key mediator of the adaptive mechanism described here. To confirm that Nrf2 mediates BZL effects we developed an Nrf2 knock-down model in HepG2 cells. Indeed, Nrf2 silencing completely prevented MRP2 induction by BZL at 24 h of incubation, definitely confirming Nrf2 mediation of the MRP2-dependent adaptive response to BZL. Furthermore, to confirm that BZL effects are not specific of HepG2 cells, we incubated primary mouse hepatocytes with BZL and evaluated ROS generation and Nrf2 nuclear translocation. Also in this model, we observed an increase in intracellular ROS and a higher Nrf2 nuclear expression after incubation with BZL, clearly indicating that the effects reported in HepG2 cells are not restricted to this experimental system (unpublished results). Finally, to evaluate whether a similar mechanism could take place *in vivo*, we treated wild type and Nrf2 knock out mice with the drug and analyzed Mrp2 expression. The results showed an increase in Mrp2 mRNA in wild type mice treated with BZL. However, BZL failed to induce Mrp2 in knock out mice, thus confirming the participation of Nrf2 in the adaptive response to BZL-triggered oxidative stress.

Our observations here, together with our previous work (Rigalli et al. 2012) support a

sequential role of Nrf2 and PXR in MRP2 up-regulation by BZL. First, BZL triggered ROS increase stimulates nuclear translocation of Nrf2, which binds to ARE elements within the MRP2 promoter, activating its transcription. Additionally, Nrf2 activates the transcription of other antioxidant systems like glutathione peroxidase that together with MRP2 counteract the oxidative insult. Once redox homeostasis is re-established, PXR activation by BZL takes place, which provides sustained MRP2 induction, even in the absence of oxidative stress (Rigalli et al. 2012). This same mechanism could be expected for other compounds that increase ROS and also activate PXR.

Our results showing no increase in SOD, CAT and GRx activities (Nrf2 target genes) at least at the time points studied here are still in line with the pattern of ROS and GSSG detoxification, but argue against antioxidant enzyme regulation by Nrf2 (Bataille and Manautou 2012; Djordjevic et al. 2015). These observations could be explained considering that transcriptional regulation by nuclear receptors is a complex mechanism involving not only activation by an agonist, but also the interplay of coactivators and corepressors that leads to an agonist-, cell type- and promoter-specific regulation. Thus, an agonist that activates a given promoter in a cell type may not necessarily activate the same promoter in another cell type (Masuyama et al. 2005). Alternatively, inhibition of antioxidant enzyme activities during BZL treatment could occur as was demonstrated for these hepatic enzymes in BZL-treated rats (Pedrosa et al. 2001). Thus, although enzyme protein levels were not assessed in this work, an induction of the expression may still be taking place, accordingly to Nrf2 activation by BZL. However, this effect may be counterbalanced by inhibition of protein activity by BZL leading to the unchanged activities observed.

In conclusion, in this work, we have shown a MRP2 driven adaptive response to BZL associated oxidative stress, being this mediated by Nrf2. These results reinforce the role of MRP2 not only facilitating the efflux of potential pro-oxidant xenobiotics but also extruding GSSG as a way to reduce the oxidative burden without consumption of NADPH. Nrf2 pharmacological activation in patients and animal models has been already report to ameliorate oxidative stress associated diseases like multiple sclerosis, skin cancer and acute kidney injury, among others.

21

Therapeutic activation of Nrf2 previous to BZL administration or potentiation of BZL-triggered Nrf2 activation might help to prevent BZL associated-oxidative stress and hepatic damage.

5. Conflict of interest

23

The authors declare that they have no conflict of interest.

6. Acknowledgements

7. References

Bataille, A.M., Manautou, J.E., 2012. Nrf2: a potential target for new therapeutics in liver disease. Clin. Pharmacol. Ther. 92, 340-348.

Biaglow, J.E., Varnes, M.E., Roizen-Towle, L. et al., 1986. Biochemistry of reduction of nitro heterocycles. Biochem. Pharmacol. 35, 77-90.

Canet, M.J., Merrell, M.D., Harder, B., Maher, J.M. et al., 2015. Identification of a Functional Antioxidant Response Element within the Eighth Intron of the Human ABCC3 Gene. Drug. Metab. Dispos. 43, 93-99.

Cantz, T., Nies, A.T., Brom, M., Hofmann, A.F., Keppler, D., 2000. MRP2, a human conjugate export pump, is present and transports fluo3 in apical vacuoles in HepG2 cells. Am. J. Physiol. Gastrointest. Liver. Physiol. 278, G522-G531.

Cichoz-Lach, H., Michalak, A., 2014. Oxidative stress as a crucial factor in liver diseases. World J. Gastroenterol. 20, 8082-8091.

Davies, C., Dey, N., Negrette, O.S., Parada, L.A., Basombrio, M.A., Garg, N.J., 2014. Hepatotoxicity in mice of a novel anti-parasite drug candidate hydroxymethylnitrofurazone: a comparison with Benznidazole. PLoS. Negl. Trop. Dis. 8, e3231.

Dias Novaes, R., Santos, E.C., Cupertino, M.C., Bastos, D.S. et al., 2015. *Trypanosoma cruzi* infection and benznidazole therapy independently stimulate oxidative status and structural pathological remodeling of the liver tissue in mice. Parasitol. Res. 114, 2873-2881.

Djordjevic, J., Djordjevic, A., Adzic, M., Mitic, M., Lukic, I., Radojcic, M.B., 2015. Alterations in the Nrf2-Keap1 signaling pathway and its downstream target genes in rat brain under stress. Brain Res. 1602, 20-31.

Dubin, M., Goijman, S.G., Stoppani, A.O., 1984. Effect of nitroheterocyclic drugs on lipid peroxidation and glutathione content in rat liver extracts. Biochem. Pharmacol. 33, 3419-3423.

25

Ferretti, A.C., Mattaloni, S.M., Ochoa, J.E., Larocca, M.C., Favre, C., 2012. Protein kinase A signals apoptotic activation in glucose-deprived hepatocytes: participation of reactive oxygen species. Apoptosis. 17, 475-491.

Fina, B.L., Lombarte, M., Rigalli, J.P., Rigalli, A., 2014. Fluoride increases superoxide production and impairs the respiratory chain in ROS 17/2.8 osteoblastic cells. PLoS. One. 9, e100768.

Frances, D.E., Ronco, M.T., Ochoa, E., Alvarez, M.L., Quiroga, A. et al., 2007. Oxidative stress in primary culture hepatocytes isolated from partially hepatectomized rats. Can. J. Physiol. Pharmacol. 85, 1047-1051.

Ghanem, C.I., Rudraiah, S., Bataille, A.M., Vigo, M.B., Goedken, M.J., Manautou, J.E., 2015. Role of nuclear factor-erythroid 2-related factor 2 (Nrf2) in the transcriptional regulation of brain ABC transporters during acute acetaminophen (APAP) intoxication in mice. Biochem. Pharmacol. 94, 203-211.

Griffith, O.W., 1980. Determination of glutathione and glutathione disulfide using glutathione reductase and 2-vinylpyridine. Anal. Biochem. 106, 207-212.

Gu, X., Manautou, J.E., 2012. Molecular mechanisms underlying chemical liver injury. Expert Rev. Mol. Med. 14, e4.

Hagmann, W., Nies, A.T., König, J., Frey, M., Zentgraf, H., Keppler, D., 1999. Purification of the human apical conjugate export pump MRP2 reconstitution and function characterization as substrate-stimulated ATPase. Eur. J. Biochem. 265, 281-289.

Hall, B.S., Wilkinson, S.R., 2012. Activation of benznidazole by trypanosomal type I nitroreductases results in glyoxal formation. Antimicrob. Agents Chemother. 56, 115-123.

Han, D., Hanawa, N., Saberi, B., Kaplowitz, N., 2006. Mechanisms of liver injury. III. Role of glutathione redox status in liver injury. Am. J. Physiol. Gastrointest. Liver Physiol. 291, G1-7.

Hariparsad, N., Chu, X., Yabut, J., Labhart, P. et al., 2009. Identification of pregnane-x-receptor

target genes and coactivator and corepressor binding to promoter elements in human hepatocytes. Nucl. Acid. Res. 37, 1160-1173.

Itoh, K., Wakabayashi, N., Katoh, Y., Ishii, T., O'Connor, T., Yamamoto, M., 2003. Keap1 regulates both cytoplasmic-nuclear shuttling and degradation of Nrf2 in response to electrophiles. Genes Cells. 8, 379-391.

Kang, K.W., Cho, I.J., Lee, C.H., Kim, S.G., 2003. Essential role of phosphatidylinositol 3-kinase-dependent CCAAT/enhancer binding protein beta activation in the induction of glutathione S-transferase by oltipraz. J. Natl. Canc. Inst. 95, 53-66.

Kast, H.R., Goodwin, B., Tarr, P.T., Jones, S.A. et al., 2002. Regulation of multidrug resistance-associated protein 2 (ABCC2) by the nuclear receptors pregnane X receptor, farnesoid X-activated receptor, and constitutive androstane receptor. J. Biol. Chem. 277, 2908-2915.

Klaassen, C.D., Aleksunes, L.M., 2010. Xenobiotic, bile acid, and cholesterol transporters: function and regulation. Pharmacol. Rev. 62, 1-96.

Lehmann, J.M., McKedd, D.D., Watson, M.A., Willson, T.M. et al., 1998. The human orphan nuclear receptor PXR is activated by compounds that regulate CYP3A4 gene expression and cause drug interactions. J. Clin. Invest. 102, 1016-1023.

Li, L., Dong, H., Song, E., Xu, X., Liu, L., Song, Y., 2014. Nrf2/ARE pathway activation, HO-1 and NQO1 induction by polychlorinated biphenyl quinone is associated with reactive oxygen species and PI3K/AKT signaling. Chem. Biol. Interact. 209, 56-67.

Lowry, O.H., Rosebrough, N.J., Farr, A.L., Randall, R.J., 1951. Protein measurement with the Folin phenol reagent. J. Biol. Chem. 193, 265-275.

Maher, J.M., Dieter, M.Z., Aleksunes, L.M., Slitt, A.L. et al., 2007. Oxidative and electrophilic stress induces multidrug resistance-associated protein transporters via the nuclear factor-E2-related factor-2 transcriptional pathway. Hepatology. 46, 1597-1610.

Masuyama, H., Suwaki, N., Tateishi, Y. et al., 2005. The pregnane X receptor regulates gene expression in a ligand- and promoter-selective fashion. Mol. Endocrinol. 19, 1170-80.

Noh, J.R., Kim, Y.H., Hwang, J.H. et al., 2015. Sulforaphane protects against acetaminophen-induced hepatotoxicity. Food Chem. Toxicol. 80, 193-200.

Pedrosa, R.C., De Bem, A.F., Locatelli, C. et al., 2001. Time-dependent oxidative stress caused by benznidazole. Redox Rep. 6, 265-70.

Perdomo, V.G., Rigalli, J.P., Villanueva, S.S.M., Ruiz, M.L., Luquita, M.G., Echenique, C.G., Catania, V.A., 2013. Modulation of biotransformation systems and ABC transporters by benznidazole in rats. Antimicrob. Agents Chemother. 57, 4894-4902.

Ramyaa, P., Krishnaswamy, R., Padma, V.V., 2014. Quercetin modulates OTA-induced oxidative stress and redox signalling in HepG2 cells - up regulation of Nrf2 expression and down regulation of NF-κB and COX-2. Biochim. Biophys. Acta. 1840, 681-692.

Reagan-Shaw, S., Nihal, M., Ahmad, N., 2008. Dose translation from animal to human studies revisited. FASEB J. 22, 659-661.

Rendon, D.A., 2014. Alterations of mitochondria in liver but not in heart homogenates after treatment of rats with benznidazole. Hum. Exp. Toxicol. 33, 1066-1070.

Rice, K.P., Penketh, P.G., Shyam, K., Sartorelli, A.C., 2005. Differential inhibition of cellular glutathione reductase activity by isocyanates generated from the antitumor prodrugs Cloretazine and BCNU. Biochem. Pharmacol. 69, 1463-1472.

Rigalli, J.P., Ruiz, M.L., Perdomo, V.G., Villanueva, S.S., Mottino, A.D., Catania, V.A., 2011. Pregnane X receptor mediates the induction of P-glycoprotein by spironolactone in HepG2 cells. Toxicology. 285, 18-24.

Rigalli, J.P., Perdomo, V.G., Luquita, M.G., Villanueva, S.S.M., Arias, A., Theile, D., Weiss, J., Mottino, A.D., Ruiz, M.L., Catania, V.A., 2012. Regulation of biotransformation systems and ABC

28

transporters by benznidazole in HepG2 cells: Involvement of Pregnane-X-Receptor. PLoS. Negl. Trop. Dis. 6, e1951.

Rigalli, J.P., Ciriaci, N., Arias, A., Ceballos, M.P., Villanueva, S.S., Luquita, M.G., Mottino, A.D., Ghanem, C.I., Catania, V.A., Ruiz, M.L., 2015. Regulation of multidrug resistance proteins by genistein in a hepatocarcinoma cell line: impact on sorafenib cytotoxicity. PLoS. One. 10, e0119502.

Sormunen, R., Eskelinen, S., Lehto, V.P., 1993. Bile canaliculus formation in cultured HEPG2 cells. Lab. Invest. 68, 652-662.

Soy, D., Aldasoro, E., Guerrero, L. et al., 2015. Population pharmacokinetics of benznidazole in adult patients with Chagas disease. Antimicrob. Agents Chemother. 59, 3342-3349.

Strauss, M., Lo Presti, M.S., Bazan, P.C. et al., 2013. Clomipramine and benznidazole association for the treatment of acute experimental Trypanosoma cruzi infection. Parasitol. Int. 62, 293-299.

Tietze, F., 1969. Enzymic method for quantitative determination of nanogram amounts of total and oxidized glutathione: applications to mammalian blood and other tissues. Anal. Biochem. 27, 502-522.

Toledo, F.D., Perez, L.M., Basiglio, C.L. et al., 2014. The Ca(2+)-calmodulin-Ca(2+)/calmodulin-dependent protein kinase II signaling pathway is involved in oxidative stress-induced mitochondrial permeability transition and apoptosis in isolated rat hepatocytes. Arch. Toxicol. 88, 1695-1709.

Viotti, R., Vigliano, C., Lococo, B. et al., 2009. Side effects of benznidazole as treatment in chronic Chagas disease: fears and realities. Expert Rev. Anti Infect. Ther. 7, 157-163.

Vollrath, V., Wielandt, A.M., Iruretagoyena, M., Chianale, J., 2006. Role of Nrf2 in the regulation of the Mrp2 (ABCC2) gene. Biochem. J. 395, 599-609.

Vyas, P.M., Roychowdhury, S., Woster, P.M., Svensson, C.K., 2005. Reactive oxygen species generation and its role in the differential cytotoxicity of the arylhydroxylamine metabolites of

sulfamethoxazole and dapsone in normal human epidermal keratinocytes. Biochem. Pharmacol. 70, 275-286.

Wardman, P., 1985. Some reactions and properties of nitro radical-anions important in biology and medicine. Environ. Health Perspect. 64, 309-320.

Winterbourn, C.C., Metodiewa, D., 1994. The reaction of superoxide with reduced glutathione. Arch. Biochem. Biophys. 314, 284-290.

Figure legends

Fig. 1. Redox status in BZL treated HepG2 cells. Indicators of intracellular redox status were determined in control and BZL-treated cells (200 µM; 15 min, 1 h, 3 h, 24 h and 48 h). tBOOH (500 µM, 15 min) was used as positive control of ROS generation. **a.** intracellular ROS, **b.** GSSG/GSSG+GSH ratio was calculated measuring from the intracellular GSSG and total glutathione (GSSG+GSH), **c.** Intracellular GSSG content. **d.** Total intracellular glutathione (GSSG+GSH). **e.** Concentration-dependence of BZL effects on intracellular redox status. GSSG/GSSG+GSH ratio was assessed after incubation with 50, 100 and 200 µM BZL (24 h). All measurements (mean ± S.D., n = 3-4) are expressed as percentage of control values (C). * different from C, $p<0.05$.

Fig. 2. MRP2 expression and MRP2 mediated GSSG efflux in BZL treated HepG2 cells. a. MRP2 expression in lysates from BZL treated cells (200 µM, 24 and 48 h). Fifteen µg of total protein were loaded in the gels. MRP2 O.D. was normalized to β-actin O.D. Uniformity of loading and transfer from gel to PVDF membrane was also determined by Ponceau S staining. Results (mean ± S.D., n = 3) are expressed as percentage of control values (C). * different from C, $p<0.05$. **b.** GSSG efflux in BZL treated cells (200 µM, 24 and 48 h). GSSG was determined in culture medium of HepG2 cells after 24 and 48 h of treatment with BZL. MK571 (10 µM) was used as MRP2 inhibitor. Experiments were performed in absence (-MK571) and presence (+MK571) of MK571. tBOOH (500 µM, 15 min) was used as a model of rapid ROS generation with increase in intracellular GSSG without MRP2 induction. Results (mean ± S.D., n = 3) are expressed as percentage of control values (C) from cells without MK571. a: different from C-MK571, b: different from BZL 24 h-MK571, c: different from BZL 48 h-MK571, d: different from tBOOH-MK571, $p<0.05$.

Fig. 3. PXR participation in MRP2 induction by BZL in HepG2 cells. HepG2 cells were transfected with a control non-silencing- (PXR^{+} cells) or with a PXR specific siRNA (PXR^{-} cells). **a.** PXR protein levels in cell lysates of PXR[+] and PXR^{-} cells were assessed through western blot. PXR O.D. was normalized to GAPDH O.D. Results (mean ± S.D., n = 3) are expressed as percentage of the ratio in PXR^{+} cells. * different from PXR[+], $p<0.05$. **b.** To further verify PXR knock-down, CYP3A4 expression was assessed through western blot in PXR[+] and PXR^{-} HepG2 cells treated with RIF (20 µM, 24 h) or vehicle (C). CYP3A4 O.D. in control and

31

RIF treated cells was normalized to GAPDH O.D. Results (mean ± S.D., n = 3) are expressed as percentage of the corresponding control. * different from control, p<0.05. **c.** MRP2 expression was quantified in total lysates of PXR$^+$ and PXR$^-$ cells exposed to BZL (200 µM, 24 h) or vehicle (C). MRP2 O.D. was normalized to GAPDH O.D. Results (mean ± S.D., n = 3) are expressed as percentage of the ratio in PXR$^+$ cells. * different from the corresponding control, p<0.05.

Fig. 4. Participation of Nrf2 in MRP2 modulation by BZL in HepG2 cells. Purity of nuclear and cytosolic fractions was checked assessing H1 Histone and GAPDH enrichment, respectively **(a)**. Nrf2 expression was quantified in nuclear extracts **(b)** and cytosolic fraction **(c)** of BZL treated HepG2 cells (200 µM; 3, 24 and 48 h). Equal amounts of protein were loaded in the gels. Nrf2 O.D. was normalized to histone H1 and GAPDH O.D. in nuclear and cytosolic fractions, respectively. Uniformity of loading and transfer from gel to PVDF membrane was also determined by Ponceau S staining. Firefly luciferase activity was assessed in HepG2 cells transfected with pGL3-ARE and exposed to BZL (200 µM; 3, 24 and 48 h) **(d)**. Results (mean ± S.D., n = 3-4) are expressed as percentage of control values (C). * different from C, p<0.05. For a final confirmation of Nrf2 participation, an Nrf2 knock-down model was established. **e:** Nrf2 expression was assessed in total lysates of Nrf2$^+$ (transfected with a non-silencing siRNA) and Nrf2$^-$ HepG2 cells (transfected with a pool of specific siRNAs against human Nrf2) and normalized to GAPDH expression. Results (mean ± S.D., n = 3) are expressed as percentage of the Nrf2/GAPDH ratio in Nrf2$^+$ cells. * different from Nrf2$^+$, p<0.05. **f:** MRP2 expression was assessed in control and BZL-treated (200 µM, 24 h) Nrf2$^+$ and Nrf2$^-$ cells. Results (mean ± S.D., n = 3) are expressed as percentage of the Nrf2/GAPDH ratio in the corresponding control cells. * different from control (C), p<0.05.

Fig. 5 Effect of BZL on hepatic Mrp2 expression in wild type and Nrf2$^{-/-}$ mice. Hepatic Mrp2 expression was quantified at the mRNA level in wild type and Nrf2 knock out control (vehicle exposed) and BZL treated mice (200 mg/kg b.w./ day, 3 consecutive days, i.p.) by real time PCR. Expression of Mrp2 (Abcc2) mRNA was normalized to β-actin mRNA. The data (mean ± S.D., n = 3) are expressed as percentage of the mRNA in the corresponding control (C) mice of each genotype. * different from the corresponding C, p<0.05.

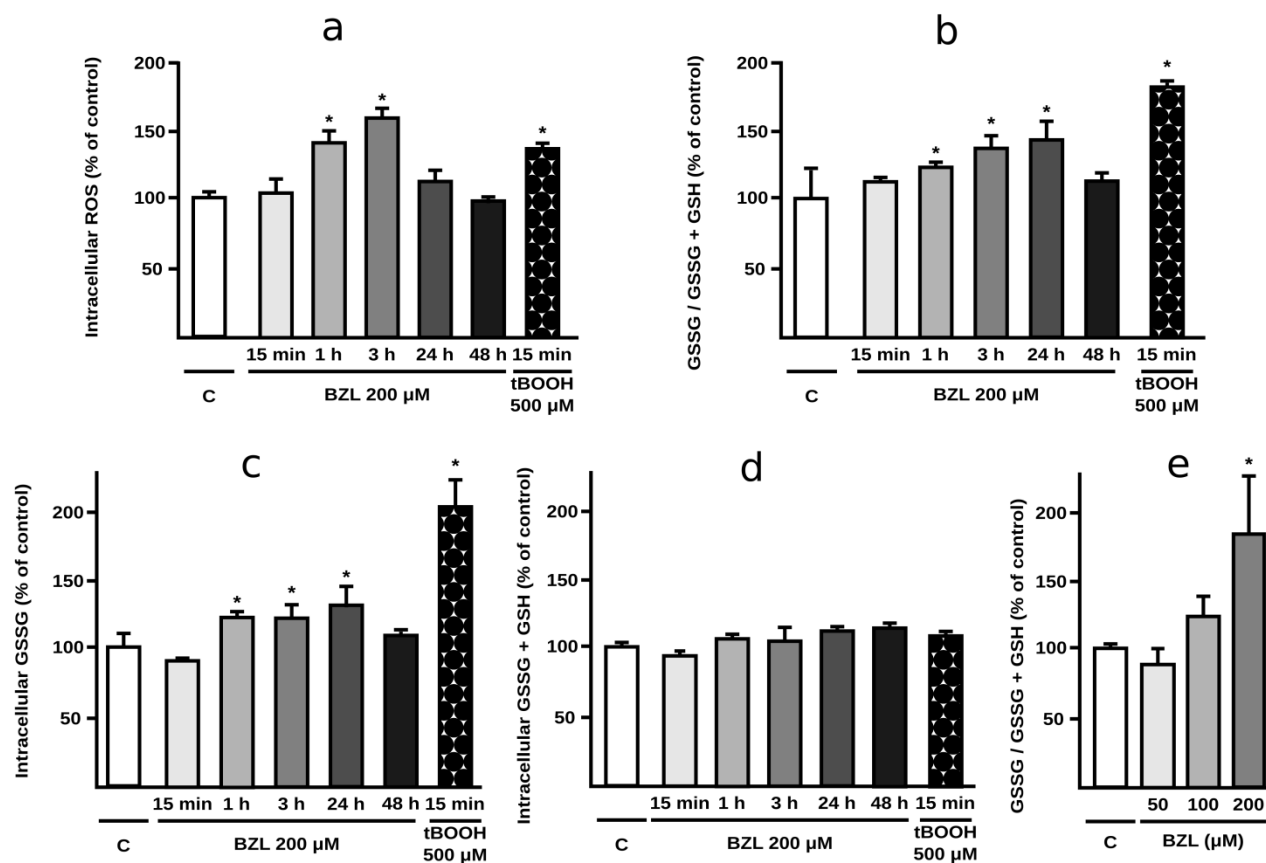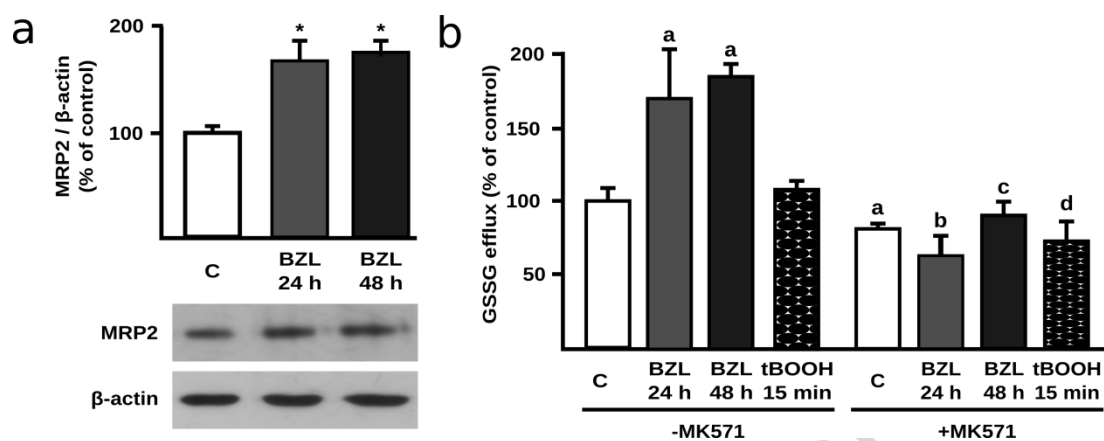**Figure 1**

Figure 2

34

Figure 3

35

a

H1 Histone

Lys Nuc Cyt

GAPDH

Lys Cyt Nuc

b

Nuclear Nrf2 / H1 Histone
(% of control)

300

200

100

C   3 h   24 h   48 h

BZL 200 μM

Nrf2

H1

c

Cytosolic Nrf2 / GAPDH
(% of control)

150

100

50

C   3 h   24 h   48 h

BZL 200 μM

Nrf2

GAPDH

d

Firefly luciferase activity
(% of control)

150

100

50

C   3 h   24 h   48 h

BZL 200 μM

e

Nrf2 / GAPDH
(% of control)

200

100

Nrf2$^+$ Nrf2$^-$

Nrf2

GAPDH

f

MRP2 / GAPDH
(% of control)

200

100

C   BZL   C   BZL

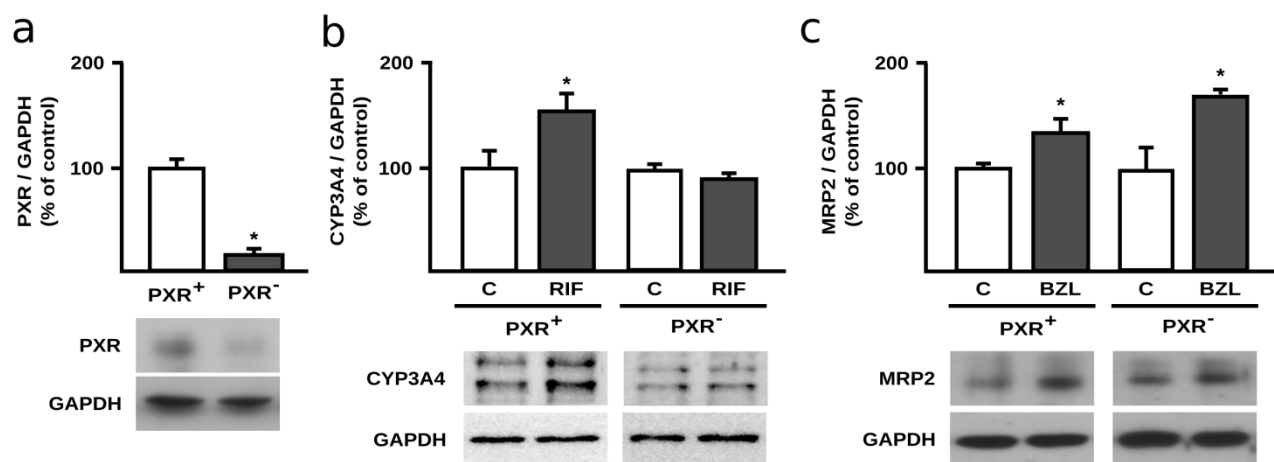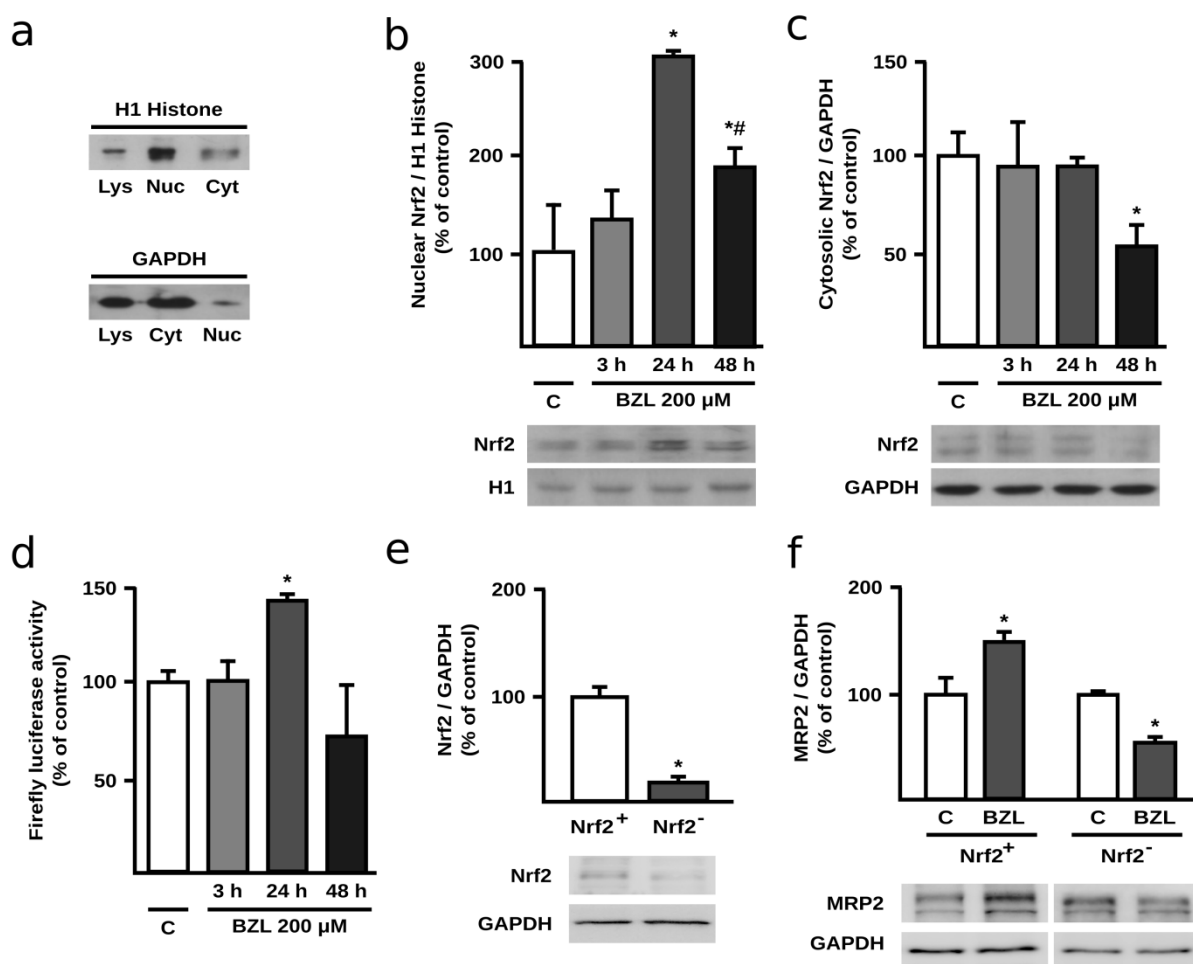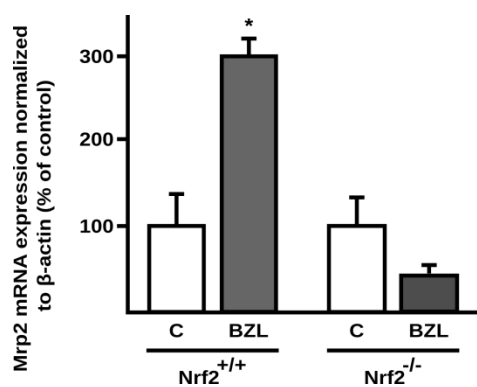Nrf2$^+$ Nrf2$^-$

MRP2

GAPDH

Figure 4

36

Figure 5

Table 1. Antioxidant enzymes in BZL treated HepG2 cells. Results are expressed as percentage of the activity measured in control cells. * different from all the other groups, $p < 0.05$, n=3. Catalase absolute activity was 1.32 ± 0.18, 0.96 ± 0.15 and 1.03 ± 0.12 µmol H_2O_2 consumed / minute . mg protein for control, BZL 12 h and BZL 24 h, respectively. Glutathione reductase absolute activity was 0.093 ± 0.009, 0.070 ± 0.020 and 0.091 ± 0.012 µmol NADPH consumed / minute . mg protein for control, BZL 12 h and BZL 24 h, respectively. Glutathione peroxidase absolute activity was 11.76 ± 0.95, 19.51 ± 1.12 and 12.46 ± 3.76 µmol NADPH consumed / minute . mg protein for control, BZL 12 h and BZL 24 h, respectively. Superoxide dismutase determinations base on a semi-quantitative method and thus, no absolute measurements can be provided.

	Control	BZL 12 h	BZL 24 h
Catalase (%)	100 ± 14	73 ± 11	78 ± 9
Superoxide dismutase (%)	100 ± 2	92 ± 24	90 ± 20
Glutathione reductase (%)	100 ± 10	75 ± 21	98 ± 13
Glutathione peroxidase (%)	100 ± 8	166 ± 10 *	106 ± 32

Highlights

- BZL triggers a redox imbalance in the human hepatic cell line HepG2.

- Concomitantly BZL triggers compensatory mechanisms to alleviate the redox injury.

- Response mechanisms comprise an enhanced glutathione peroxidase and MRP2 activity.

- Transcription factor Nrf2 plays a key role orchestrating compensatory mechanisms.